RSC Advances

This article can be cited before page numbers have been issued, to do this please use: S. CHEN, C. Karuppiah, M. K, A. A. M, S. Palanisamy, R. A, P. Periakaruppan, A. Fahad M.A. and B. Lou, *RSC Adv.*, 2015,

ROYAL SOCIETY OF CHEMISTRY

www.rsc.org/advances

View Article Online
DOI: 10.1039/C5RA00992H

Journal Name

RSCPublishing

ARTICLE

Cite this: DOI: 10.1039/xoxxoooooox

Green synthesized silver nanoparticles decorated on reduced graphene oxide for enhanced electrochemical sensing of nitrobenzene in waste water samples

K. Chelladurai, [a] K. Muthupandi, [b] S.M. Chen, [a, c*] M. Ajmal Ali, [c] P. Selvakumar, [a] A. Rajan, [b] P. Prakash, [b**] Fahad M. A. Al-Hemaid, [c] Bih-Show Lou[d***]

Received ooth January 2012,
Accepted ooth January 2012

DOI: 10.1039/xoxxoooooox

www.rsc.org/

In the present work, an electrochemical sensor for nitrobenzene has been developed based on green synthesized silver nanoparticles (AgNPs) decorated reduced graphene oxide (RGO) modified glassy carbon electrode (GCE). The AgNPs were synthesized using *Justicia glauca* leaf extract as a reducing and stabilizing agent. RGO-AgNPs composite modified electrode was prepared by a simple electrochemical reduction of AgNPs dispersed GO solution. FESEM of RGO-AgNPs composite confirms that AgNPs are firmly attached on the RGO sheets and the average size of AgNPs is found to be 40 ± 5 nm**.** The modified electrode shows good efficiency with lower overpotential for electrocatalytic reduction of NB than that of other modified electrodes (AgNPs and RGO). The DPV response confirms that the reduction peak current of NB is linear over the concentrations from 0.5 to 900 μM. The sensitivity of the sensors is found to be 0.836 $\mu A \mu M^{-1}$ cm^{-2} with the detection limit of 0.261 μM for NB. In addition, the RGO-AgNPs composite modified electrode shows good selectivity in the presence of potentially interfering similar compounds and good practicality in the waste water samples.

1. Introduction

Nitrobenzene (NB) is a highly toxic carcinogenic compound and has been listed as one of the priority pollutants by United States Environmental Protection Agency (USEPA).[1] It has also been used as a raw material for the preparation of explosives, herbicides, insecticides, aniline and dyes.[2–4] Even in very low concentration, the NB may pose great threat to human health and environment. Large amount of NB is released from the industries and resulting in high toxicity of water bodies. It is very stable in aqueous solution due to the presence of NO_2 group.[5–7] Therefore, the sensitive determination of NB in environmental samples is of great importance for human health. The well known methods for NB determination are based on chromatographic, spectrophotometry and electrochemical methods.[8–10] In recent years, electrochemical methods are widely used for the quantitative determination of NB due to their high sensitivity, easy handling and low cost.[11]

ARTICLE View Article Online DOI: 10.1039/C5RA00992H Journal Name

Compared to unmodified electrodes, the nanomaterials modified electrodes have been widely used for the electrochemical determination of NB owing to their high surface area and excellent electrochemical property.[12] In addition, these modified electrodes enhance the sensitivity and selectivity of the NB detection more than that of conventional electrodes. Researchers have paid much attention on reduced graphene oxide (RGO) owing to its unique properties such as high specific surface area and high chemical stability.[13–15] The unique properties of RGO combined with other nanomaterials have been used for different potential applications, such as energy storage, antibacterial, electrochemical sensor and biosensors, gas sensors etc.[16–23] Among the variety of metal and metal oxide nanoparticles, AgNPs have received considerable interest due to their unique structural properties including sensing of nitro compounds.[24–27] Recently, our group has found that the green synthesized nanoparticles have high electrocatalytic activity towards NB.[27] However, the green synthesized AgNPs have some limitations on the detection of nitro compounds, such as low sensitivity, lower response range and narrow potential window. In order to improve the sensitivity, the AgNPs have been combined with RGO and used for the ultrasensitive detection of NB.

Herein, we report the electrochemical determination of NB using AgNPs decorated RGO (RGO-AgNPs) modified glassy carbon electrode (RGO). The modified electrode exhibits good sensitivity and lower overpotential compared to AgNPs and RGO modified electrodes. Moreover, the analytical performance of the modified electrode has been evaluated in waste water samples and the selectivity of the fabricated sensor has also been determined in the presence of potentially interfering compounds such as nitro and phenolic compounds and metal ions.

2. Experimental

Materials

Silver nitrate ($AgNO_3$) and nitrobenzene were purchased from Sigma–Aldrich. The leaves of *Justicia glauca* were collected from Sirumalai hills region, Tamil Nadu, India. Raw graphite with average diameter about >20 μm was obtained from Sigma Aldrich. The supporting electrolyte used for all experiments was prepared by using 0.05 M Na_2HPO_4 and NaH_2PO_4 solutions. All other chemicals were of analytical grade and the solutions were prepared with double-distilled water.

Methods

Cyclic voltammetry (CV) and differential pulse voltammetry (DPV) experiments were carried out using CHI 750a work station. A conventional three-electrode cell containing the modified GCE was used as a working electrode. Pt wire and saturated Ag/AgCl were used as a counter and reference electrodes, respectively. Surface morphological study was carried out using JSM-6500F field emission scanning electron microscope (FESEM) and the elemental analysis was performed using Hitachi S-3000 H scanning electron microscope attached with Energy Dispersive X-ray Analyzer. Jasco V-560 double-beam spectrophotometer was used for UV–visible spectral analysis. All the electrochemical measurements were carried out at room temperature in a nitrogen (N_2) atmosphere.

Green synthesis of AgNPs

The 50 mL of *Justicia glauca* leaf extract was mixed with 100 mL of aqueous solution of 1 mM $AgNO_3$ at room temperature. The pale greenish yellow colour solution becomes deeper brown within an hour and no noticeable difference in the colour of aqueous silver colloids is observed, which indicates that the bio-reduction process is over within an hour. The colour changes indicate the formation of AgNPs in aqueous solution due to excitation of Surface Plasmon vibration in the metal nanoparticles as shown in **Fig. S1**. The synthesized AgNPs were collected by centrifugation and washing several times with double distilled water. The dried AgNPs

View Article Online
DOI: 10.1039/C5RA00992H ARTICLE

were lyophilized in ambient condition. After lyophilisation, the AgNPs were stored in screw cap bottle for further characterization.

Fabrication of RGO-AgNPs modified GCE

The GO was synthesized according to our previous report using Hummers method.[24] 1 mgmL^{-1} of GO solution was taken to synthesize the present nanocomposite. In order to prepare the RGO-AgNPs composite, the as-synthesized AgNPs with different concentrations (0.5, 1, 2 and 3 mg mL^{-1}) were mixed with GO (1 mg mL^{-1}) solution and sonicated for 30 min. About 6 µL (optimum) of GO/AgNPs solution was drop casted on pre-cleaned GCE surface. 10 consecutive cyclic voltammograms were performed using the GO/AgNPs modified electrode in the potential range of 0 to -1.3 V in pH 5 solution at a scan rate of 50 mV s^{-1}. After 10 successive consecutive cycles the GO/AgNPs modified electrode was reduced to RGO-AgNPs modified electrode.[28] The resulting RGO-AgNPs modified electrode was further used for the detection of NB.

3. Results and Discussion

Characterization of synthesized RGO-AgNPs composite

UV–Vis spectroscopy is an important technique to verify the size, shape, and stability of the nanoparticles. The formation of AgNPs was visually identified by means of change in colour from pale greenish yellow to brown.[29] **Fig. S1** illustrates the UV–Vis spectra of silver colloid with different time intervals of 10, 30, 60 min. The spectral values were recorded at 445, 452, 453 nm and they were indexed as S_1, S_2, S_3, respectively. The SPR peak occurs at 453 nm with high absorbance for AgNPs.[30] The absorption peak steadily increases and after 1 h there is no increase in the absorption peak, which confirms that the reaction is completed within 1 h. The intensity of colour does not intensify after 1 h which is established by UV–Vis spectra. The size and morphology of the synthesized Ag-NPs on RGO were determined by FESEM. **Fig. 1** displays the FESEM image of AgNPs (A), GO-AgNPs (B) and RGO-AgNPs (C).

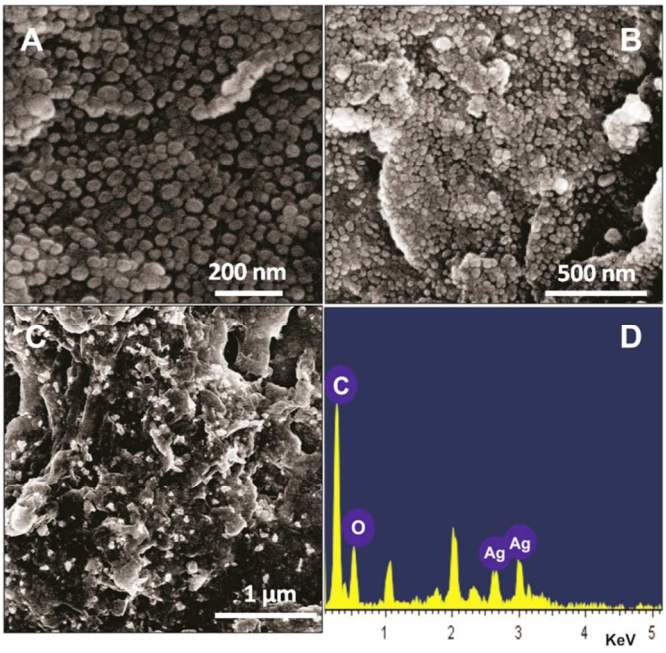

Fig. 1 FESEM images of AgNPs (A), GO-AgNPs (B) and RGO-AgNPs (C). The corresponding EDX of RGO-AgNPs.

As shown in Fig. 1C, the spherical and uniform sized AgNPs are observed on RGO. The morphology and size of the AgNPs are in close agreement with the AgNPs on GO (B). The EDX results also further confirm the presence of metallic Ag, carbon and oxygen in the RGO-AgNPs composite. The particle size distribution histogram for AgNPs in GO-AgNPs and RGO-AgNPs composites are shown in Fig. 2A and B. The histogram of AgNPs in RGO-AgNPs composite indicates that the size of the AgNPs is 40 nm and the observations are in close agreement with the size of AgNPs in RGO. These findings further confirm that the size of the AgNPs is not affected after the electrochemical preparation of RGO-AgNPs.

Raman spectroscopy is widely used for the confirmation of the transformation of GO to RGO. Fig. 2C shows the Raman spectra of GO (black line), RGO (brown line) and RGO-AgNPs (blue line). The Raman spectra of GO, RGO and RGO-AgNPs show the D and G band at about 1338 and 1509 cm^{-1}, 1339 and 1606 cm^{-1} and 1339

View Article Online
DOI: 10.1039/C5RA00892H
Journal Name

and 1608 cm^{-1}, respectively. The D and G bands are attributed to the vibrations of sp^3 carbon atoms of disordered graphene nanosheets and vibrations of sp^2 carbon atom domains of graphite. The RGO and RGO-AgNPs show higher intensity (1.06) of the D to G band (I_D/I_G) than that of GO (1.0). The result indicates that the high ability for the recovery of the hexagonal network of carbon atoms and formation of new graphitic domains. Furthermore, the observed intensity of the G band of RGO-AgNPs is higher than RGO, which is attributed to the polar interaction of AgNPs with RGO. However, the interaction of AgNPs with RGO is relatively low compared to GO due to the less oxygen-containing groups of RGO. These observations further confirm the transformation GO-AgNPs to RGO-AgNPs after the electrochemical reduction process.

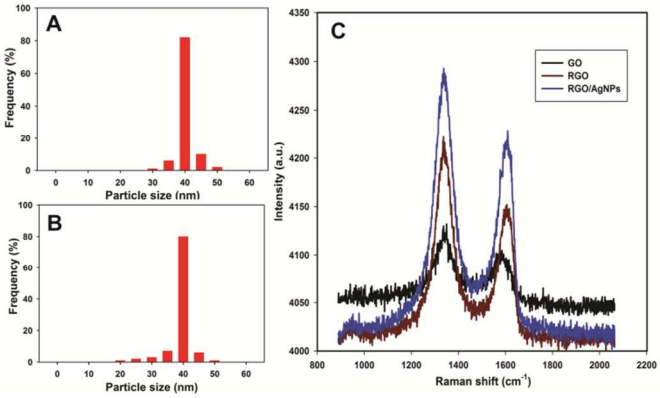

Fig. 2 The size distribution histogram of AgNPs in GO-AgNPs (A) and RGO-AgNPs (B). (C) Raman spectra of GO (black line), RGO (brown line) and RGO-AgNPs (blue line).

Fig. S2 shows the spectra obtained from the powdered samples of untreated leaf (b) and green synthesized AgNPs (a), respectively. The band around 3752 and 3652 cm^{-1} can be assigned to the –C– of carboxylic group.[29] Band around 3569 and 3371 cm^{-1} can be assigned for the O–H stretching vibration indicating the presence of hydroxyl group.[30] The minor as well as sharp band observed in the region 2925 and 2850 cm^{-1} is due to the stretching vibration of -C–H–.[31] The band observed at 1741 cm^{-1} is attributed to a carbonyl group. The strong as well as broad band observed at1649 cm^{-1} may be assigned to the -OH bending modes. The band observed at 1514 cm^{-1} is assigned to C- C aromatic vibrations.[32] The weak band observed at 1400 cm^{-1} is due to C–H deformation vibrations. The band observed at 1153 cm^{-1} can be attributed to carbonyl group as in aldehydic or ketonic group. The band observed at 1028 cm^{-1} is due to the vibrational stretching frequency modes of C–O–C of phenolic compounds.[33] After the bioreduction of silver ion with the *Justicia glauca* extract, the bands at 3652, 3752 and 3569 cm^{-1} remain unaffected but the band intensities have reduced. It suggests the possible involvement of –C– of carboxylic group and hydroxyl group during the nanoparticles synthesis. The band at 3371 cm^{-1} is shifted to 3429 cm^{-1} with broad band intensity, suggesting that the hydroxyl group plays a vital role during the nanoparticles synthesis. The sharp band at 2925 cm^{-1} and minor band at 2850 cm^{-1} are unaffected but the band intensities have decreased. This suggests the possible involvement of -C–H– of aromatic ring during the nanoparticles synthesis. The band at 1741 cm^{-1} is shifted to 1751 cm^{-1}, suggesting the possible involvement of carbonyl group in the nanoparticles synthesis. The sharp and narrow band at 1649 cm^{-1} is shifted to 1697 cm^{-1} with diminished band intensity, suggesting that the excess of hydroxyl groups in aromatic ring involve throughout the nanoparticles synthesis. The sharp and narrow band at 1514 cm^{-1} is shifted to 1600 cm^{-1} with reduced band intensity, confirming the possible involvement of C- C aromatic group during the synthesis. The band at 1400 cm^{-1} is shifted to 1425 cm^{-1} with reduced band intensity, suggesting the involvement of C–H group in aromatic ring. The band at 1153 cm^{-1} remains unaffected but the band intensity has reduced, which suggests the possible involvement of carbonyl group. The broad band at 1028 cm^{-1} is shifted to 1018 cm^{-1} with reduced band intensity, suggesting the involvement of C–O–C of phenolic compound during the bioreduction process.[34–36]

Electrochemical properties of RGO-AgNPs composite

View Article Online
DOI: 10.1039/C5RA00992H ARTICLE

To evaluate the electrochemical properties of RGO-AgNPs composite, cyclic voltammetry was performed in a 5 mM $K_3[Fe(CN)_6]$ solution with 0.1 M KCl at a scan rate of 100 mV s^{-1}. **Fig. 3A** represents the electrochemical behaviour of redox couple of Fe(III)/Fe(II) at bare GCE (a), GO-AgNPs/GCE (b) and RGO-AgNPs/GCE (c). At bare GCE, a well-defined redox peaks appear with a peak-to-peak separation (ΔE_p) of 136 mV, which indicates that the electrochemical process of Fe(III)/Fe(II) at bare GCE is reversible.

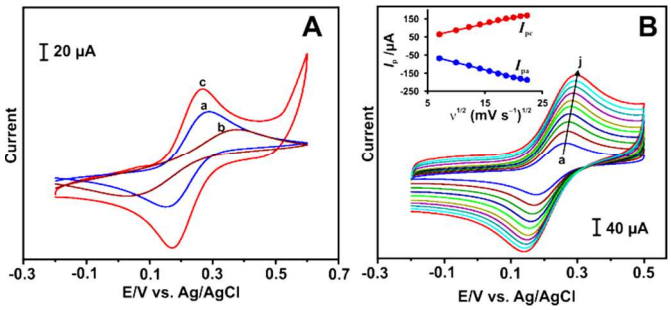

Fig. 3 A) CV response of bare GCE (a), GO-AgNPs/GCE (b) and RGO-AgNPs/GCE (c) in 5 mM $K_3[Fe(CN)_6]$ solution with 0.1 M KCl at a scan rate of 100 mV s^{-1}. B) CV response of RGO-AgNPs modified GCE in 5 mM $K_3[Fe(CN)_6]$ solution with 0.1 M KCl at different scan rates from 50 to 500 mV s^{-1} (a–j).

In contrast, the current intensities decrease with higher ΔE_p (374 mV) observed at GO-AgNPs/GCE, which is attributed to the low surface area that retards the electrochemical activity of GO-AgNPs. However, the Fe(III)/Fe(II) redox couple is highly active on RGO-AgNPs/GCE with increased peak current response with low ΔE_p (97 mV). This result indicates that the electron transfer kinetics of Fe(III)/Fe(II) is greatly enhanced by RGO-AgNPs composite compared to other modified electrodes. This is because of the high conductivity of RGO-AgNPs thus improving the electron transfer of redox couple towards electrode surface. In addition, CVs were also recorded for the influence of scan rate at the RGO-AgNPs/GCE under similar experimental conditions and are shown in **Fig. 3B**. The redox peak current of Fe(III)/Fe(II) increases with increasing the scan rate from 50 to 500 mV s^{-1}, and the anodic and cathodic peak currents are linear with the square roots of the scan rates (**Fig. 3B inset**). This result indicates that the electrochemical behaviour of Fe(III)/Fe(II) at the modified electrode is a typical diffusion controlled electrochemical process.

Electrochemical behaviour of NB on RGO-AgNPs modified electrode

The electrochemical behaviour of NB on different modified electrodes was studied by using CV. **Fig. 4A** depicts the electrochemical behaviour of NB on (a) bare, (b) AgNPs, (c) GO, (d) RGO, (e) GO-AgNPs, (g) RGO-AgNPs modified GCEs in 100 µM NB containing PBS at a scan rate of 50 mV s^{-1}. As can be seen in curve f (RGO-AgNPs), there is no significant peak appeared in the absence of 100 µM NB, whereas a well-defined reduction peak (R_1) is clearly observed at -0.458 V in the presence of 100 µM NB (curve g). The corresponding peak is related to the reduction of NB to phenyl hydroxylamine. Although three more peaks are observed at RGO-AgNPs modified GCE and designated as R_2, R_3 and O_1. The peak R_2 is due to the formation of aniline from phenyl hydroxylamine (R_1) and the redox peak R_3/O_1 is the reversible behaviour of phenyl hydroxylamine to nitrosobenzene.[37] The peak current of R_2 is lower than R_1, which indicates that the NB reduction at RGO-AgNPs/GCE is more favoured to form a phenyl hydroxylamine in neutral or alkaline medium. On the other hand, the enhanced reduction peak current response is observed on RGO-AgNPs modified GCE compared to other modified GCEs. Moreover, the reduction peak potential of NB shifts toward positive direction at RGO-AgNPs modified electrode by 151, 276, 255 and 250 mV compared to GO-AgNPs (e), RGO (d), AgNPs (b) and (a) bare GCEs, respectively. The result demonstrates that the decrease in overpotential of RGO-AgNPs electrode toward NB is attributed to

View Article Online
DOI: 10.1039/C5RA00092H
Journal Name

the strong π–π interaction between the NB and RGO and more active sites of AgNPs.[38] The firm attachment of AgNPs on RGO nanosheets is due to the polar interaction of AgNPs with oxygen functional groups of RGO.

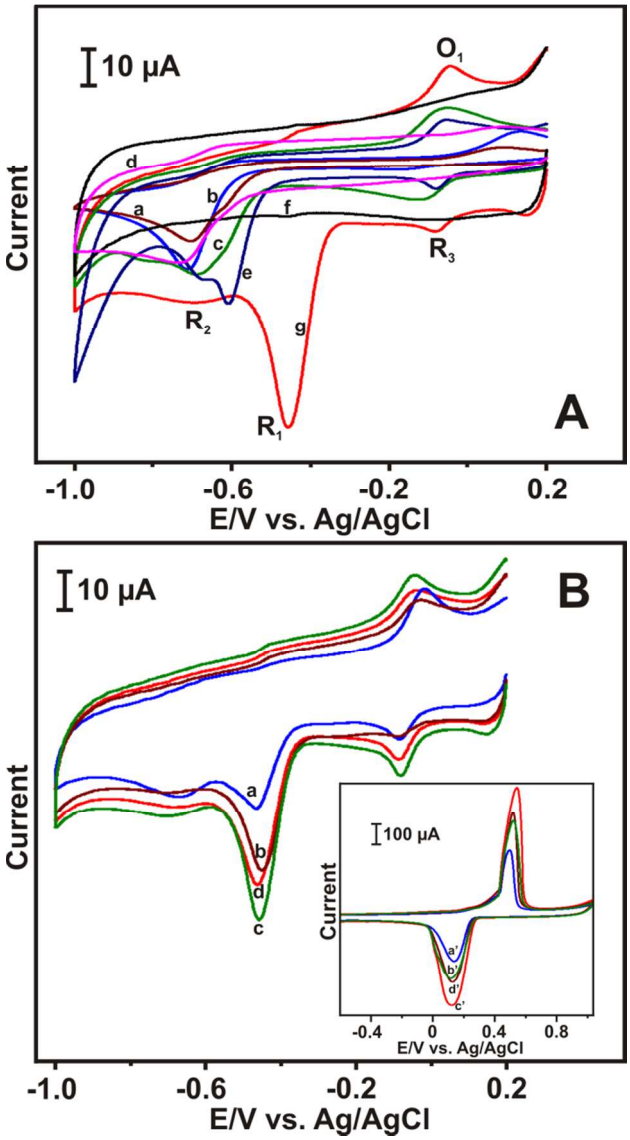

Fig. 4 A) CVs obtained at (a) bare, (b) AgNPs, (c) GO, (d) RGO, (e) GO-AgNPs, (g) RGO-AgNPs modified GCEs in 100 μM NB containing PBS at a scan rate of mVs^{-1}. At same conditions, RGO-AgNPs modified GCEs in the absence of 100 μM NB (f). B) CV response of different concentrations of AgNPs (0.5, 1, 2 and 3 mg/mL; curve a–d) at RGO-AgNPs modified GCE in 100 μM NB containing PBS at a scan rate of 50 mVs^{-1}. Inset; CV response of RGO-AgNPs modified GCE with the different concentration of AgNPs (0.5, 1, 2 and 3 mg/mL; curve a'–d') at RGO-AgNPs modified GCE in PBS at a scan rate of 50 mVs^{-1}.

The effect of different concentrations of AgNPs on the electrochemical response of NB in RGO was further studied by using CV. The different concentrations of GO-AgNPs dispersions were prepared by dispersing AgNPs (0.5, 1, 2 and 3 mg/mL) in GO solution by sonication. **Fig. 4B** shows the CV response of 100 μM NB containing PBS at different concentrations of AgNPs loaded RGO modified electrode at a scan rate of 50 mV s^{-1}. The utmost cathodic peak current response is observed for 2 mg/mL AgNPs dispersed RGO. As shown in **Fig. 4B** inset, the maximum anodic and cathodic peak current of AgNPs at RGO is observed for 2 mg/mL AgNPs dispersion. The current response of AgNPs decrease in the concentration of AgNPs above or below 2 mg/mL dispersion. Hence 2 mg/mL AgNPs dispersed GO solution was used for the RGO-AgNPs electrode fabrication and chosen as an optimum for further electrochemical studies for NB.

Fig. 5A shows the CV responses of RGO-AgNPs modified electrode in 100 μM NB containing PBS at a scan rate of 50 mV s^{-1}. The reduction peak current of NB increases with increasing the scan rates from 20 to 200 mVs^{-1} (a–j) and the peak potential (E_{pc}) shifts slightly towards negative potential. The reduction peak current response of NB has a linear relationship with the square root of scan rates (**Fig. 5A inset**). The linear regression equation is found to be Ip (μA) = 1.2798 $\nu^{1/2}$ $(mVs^{-1})^{1/2}$ + 5.5565; R^2 = 0.9938. The result indicates that the electrochemical reduction of NB at RGO-AgNPs/GCE is a diffusion controlled irreversible electrode process. The irreversible electrochemical behaviour NB is confirmed from the plot of E_{pc} vs. logν (**Fig. S3**) and the corresponding linear regression equation can be expressed as, E_{pc} (V) = –0.0899 logν – 0.2858; R^2 = 0.9983. According to the Tafel equation, the above

Journal Name
View Article Online
DOI: 10.1039/C5RA00992H
ARTICLE

relationship can be expressed as:

$$E_{pc} = -\frac{2.303RT}{2\alpha nF} log + K \quad (1)$$

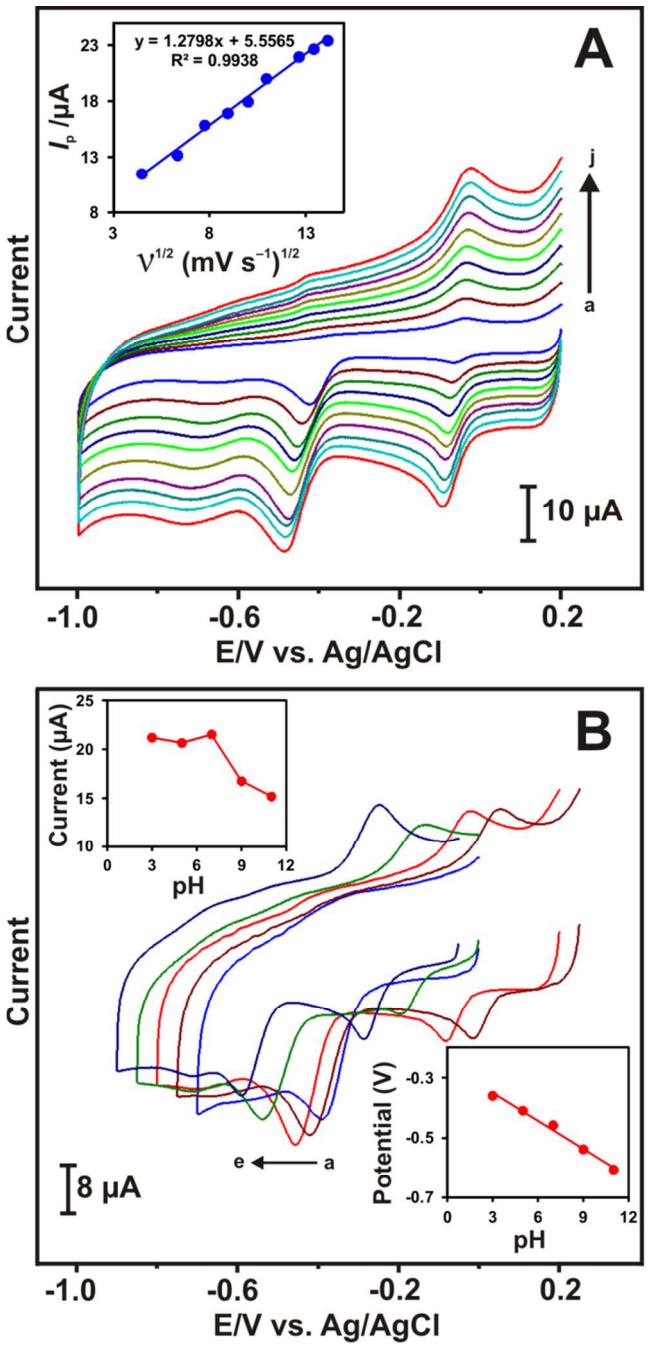

Fig. 5 A) CV response of RGO-AgNPs/GCE in 100 μM NB containing PBS at different scan rates range from 20 to 200 mVs^{-1} (a–j) and inset shows the plot of I_{pc} vs. square roots of scan rates. B) CV response for 100 μM NB at RGO-AgNPs/GCE in different pH solutions from 3 to 11(a–e). Upper inset: the plot of I_{pc} vs. pH; Lower inset: the E_{pc} vs. pH.

Where, R is the gas constant (8.314 JK^{-1} mol^{-1}), T is the room temperature (298 K), α is the electron transfer coefficient, n is the number of electrons transferred and F is the Faraday's constant (96485 C mol^{-1}) and α value is calculated as 0.66. The Tafel slope, b = 2.303RT/αnF, value is calculated to be 89.9 mV/decade which is higher than 60 mV.[39, 40] The obtained b value clearly indicates that one electron is involved in the rate determining step. The electrochemical reduction of NB is evaluated by CV at RGO-AgNPs modified electrode in the presence of 100 μM NB containing different pH solutions (pH 3, 5, 7, 9 and 11,(a–e)) as depicted in **Fig. 5B**. Upon increasing the pH from 3 to 7 (upper inset), the I_{pc} increases gradually up to 7 and then decreases at higher pH with negative potential shift (lower inset). This result suggests that the electrochemical reduction of NB is pH dependent and hydrogen ion concentration may affect the rate of reduction reaction. In addition, the reduction product of NB, phenyl hydroxylamine, is more active in neutral and/or higher pH range.[41] Hence, the pH 7 was chosen as an optimum pH for further analytical studies of NB.

Electrochemical determination of NB RGO-AgNPs modified electrode

The electrochemical determination of NB was done at RGO-AgNPs modified electrode in PBS by using DPV. **Fig. 6** depicts DPV response of RGO-AgNPs modified electrode in different concentrations of NB from 0.5 to 900 μM (a–r) containing PBS. It can be seen that a sharp reduction peak is observed for the addition of 0.5 μM NB and the reduction current increases with increasing the concentration of NB. The reduction peak current response increases linearly up to 900 μM (**Fig. 6B inset**). The calibration plot for I_{pc} versus different concentrations of NB is found to be I_{pc} = 0.0663 [NB]/μM + 1.5981 with the correlation coefficient

View Article Online
DOI: 10.1039/C5RA00092H
Journal Name

of 0.9965. The sensitivity is calculated as 0.836 μAμM^{-1} cm^{-2}. The limit of detection (LOD) is estimated to be 0.261 μM.

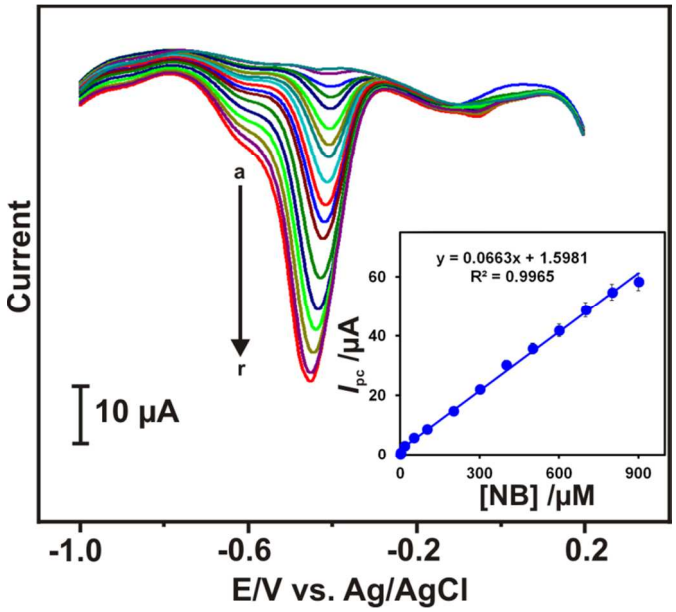

Fig. 6 DPV response of RGO-AgNPs/GCE for PBS containing different concentrations of NB in the concentration range of 0.5–900 μM (a–r). Inset: the calibration plot of I_{pc} vs. [NB]/μM

The analytical performance such as LOD, sensitivity, linear response range of the sensor was compared with previously reported NB sensors and the comparative results are shown in Table 1. It can be seen that the developed NB is more comparable with the previously reported NB sensors.[42–48] Thus, it can be used for sensitive detection of NB in environment samples.

Selectivity study

In order to study the effect of interference, the DPV was performed at RGO-AgNPs modified electrode for the response of 100 μM NB in the presence of different nitroaromatic compounds and some potentially interfering metal ions. **Fig. 7** represents the percentage of relative error for the determination of NB with 5-fold of organic and 10-fold of metal ions, such as 4-bromo nitrobenzene (4-Br NB), 4-chloro nitrobenzene (4-Cl NB), 4-nitroaniline (4-NA), 4-nitrobenzoic acid (4-NBA), 4-acetamido phenol (4-AP), 4-nitro phenol (4-NP), 4-nitro toluene (4-NT), cadmium (Cd^{2+}) and lead (Pb^{2+}) respectively. The nitroaromatic compounds such as 4-Br NB, 4-Cl NB, Cd^{2+} and Pb^{2+} show less interfering effect of about 3.6 % on the NB detection.

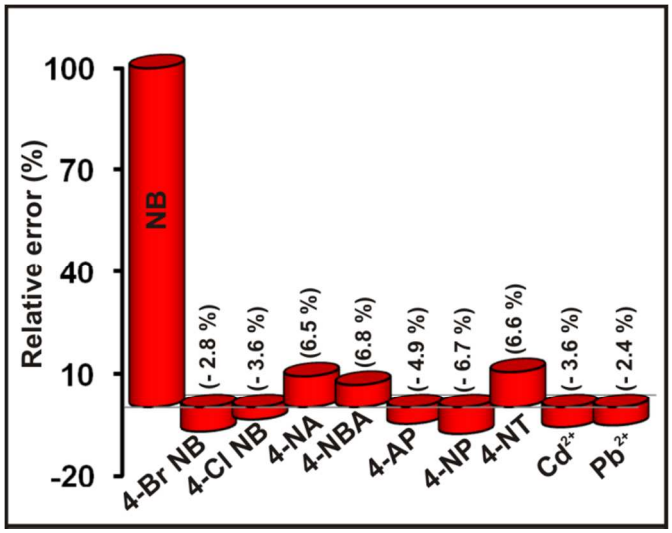

Fig. 7 Effect of addition of 5 fold interference species on the cathodic peak current response of 100 μM NB at RGO-AgNPs/GCE. Tested interfering species (x axis); 4-bromo NB (4-Br NB), 4-chloro NB (4-Cl NB), 4-nitroaniline (4-NA), 4-nitrobenzoic acid (4-NBA), 4-acetamido phenol (4-AP), 4-nitro phenol (4-NP) and 4-nitro toluene (4-NT); 10-fold of cadmium (Cd^{2+}) and lead (Pb^{2+}). Peak current response of 100 μM NB changed (y axis).

Whereas the other nitroaromatic compounds significantly affect the peak current response of NB owing to their similar structural activity, the response current of NB is changed only 6.8 % in the presence 5-folds concentration of nitroaromatic compounds, which indicate that the fabricated modified electrode is more suitable for selective determination of NB in the presence of nitroaromatic compounds and metal ions.

Determination of NB in real sample analysis

The practical viability of the fabricated RGO-AgNPs modified electrode was evaluated for the determination of NB in waste water samples. The waste water samples were collected from

View Article Online
DOI: 10.1039/C5RA00992H ARTICLE

outside the university premise. The DPV was used for the determination of NB and the waste water did not show any response for NB, which reveals that no NB contamination was found in the collected waste water samples. Under similar experimental conditions, the different concentration of NB was spiked into the waste water samples and the recovery results were calculated by the standard addition method. The recovery result along with relative standard deviation (RSD) is summarized in Table **2.** The good recovery results with a range of about 98.2 – 100.8 % is obtained using the fabricated electrode and the RSD values for three samples are of 2.96, 2.63 and 3.22 %, respectively. These good recovery results and RSDs of the developed sensor prove the good practicality towards the determination of NB in waste water samples.

Stability, repeatability and reproducibility studies

The electrode stability is most significant factor for all newly developed sensors. The reduction peak current response of 100 μM NB at RGO-AgNPs modified electrode was examined up to 52 days by CV and stored in PBS when not in use. The modified electrode retains about 90.15 % of its initial current response after 52 days, which indicates the excellent storage stability of the sensor. To evaluate the repeatability and reproducibility of the developed sensor, the CVs were performed for the reduction of 100 μM NB in PBS. The acceptable repeatability with the RSD of 4.2 % is found for single electrode in 5 different measurements. The fabricated sensor shows a satisfactory reproducibility with the RSD of 3.80 % for determination of NB using 5 different sensors.

4. Conclusions

In conclusion, green synthesized AgNPs decorated RGO modified GCE has been used for the sensitive detection of NB. The RGO-AgNPs modified electrode exhibits a high sensitivity and lower overpotential for the detection of NB compared to other modified electrodes. The fabricated electrode shows many advantages, such as good sensitivity, low LOD, wide linear response range along with good selectivity for NB determination. A good recovery result of NB in waste water samples indicates the good practicality of the developed sensor. The fabricated sensor can be further extended for the sensitive trace level detection of NB in environmental samples.

Acknowledgments

The support of the visiting professorship to SMC at the King Saud University is gratefully acknowledged.

Notes and references

[a]Electroanalysis and Bioelectrochemistry Lab, Department of Chemical Engineering and Biotechnology, National Taipei University of Technology, No. 1, Section 3, Chung-Hsiao East Road, Taipei 106, Taiwan, ROC. E-mail: smchen78@ms15.hinet.net;

Fax: +886-2-27025238; Tel: +886-2-27017147.

[b]Department of Chemistry, Thiagarajar College, Madurai-625009, Tamilnadu, India

E mail: kmpprakash@gmail.com;

Fax: +91-4522312375, Tel: +91-9842993931, +91-4522456783.

[c]Department of Botany and Microbiology, College of Science, King Saud University Riyadh 11451, Saudi Arabia

[d]Chemistry Division, Center for General Education, Chang Gung University, Tao-Yuan, Taiwan. E-mail: blou@mail.cgu.edu.tw

1. A. Agrawal and P.G. Tratnyek, Environ. Sci. Technol., 1996, **30**, 153–160.
2. Y. Mu, H.Q. Yu, J.C. Zheng, S.J. Zhang and G.P. Sheng, Chemosphere, 2004, **54**, 789–794.
3. A. Zosel, K. Rychter and J.B. Leikin, Am. J. Ther., 2007, **14**, 585–587.
4. L. Zhao, J. Ma and Z.Z. Sun, Appl. Catal. B: Environ., 2008, **79**, 244–253.
5. B.E. Haigler, J.C. Spain, Appl. Environ. Microbiol., 1991, **57**, 3156–3162.

View Article Online
DOI: 10.1039/C5RA00992H
Journal Name

6. P.S. Majumder and S.K. Gupta, Water Res., 2003, **37**, 4331–4336.
7. P. Roy, A.P. Periasamy, C.T. Liang, H.T. Chang, Environ. Sci. Technol., 2013, 47, 6688–6695.
8. S.P. Wang and H.J. Chen, J. Chromatogr. A, 2002, **979**, 439–446.
9. H. Ebrahimzadeh, Y. Yamini and F. Kamarei, Talanta, 2009, **79**, 1472–1477.
10. Y. Mu, R.A. Rozendal, K. Rabaey and J. Keller, Environ. Sci. Technol., 2009, **43**, 8690–8695.
11. Y. Zhang, L. Zeng, X. Bo, H. Wang and L. Guo, Anal. Chim. Acta, 2012, **752**, 45–52.
12. J. Tang, D.P. Tang, Q.F. Li, B.L. Su, B. Qiu, G.N. Chen, Anal. Chim. Acta, 2011, **697**, 16–22.
13. A.K. Geim and K.S. Novoselov, Nat. Mater., 2007, **6**, 183–191.
14. M. Pumera, A. Ambrosi, A. Bonanni, E.L.K. Chng and H.L. Poh, Trends Anal. Chem., 2010, **29**, 954–965.
15. V. Singh, D. Joung, L. Zhai, S. Das, S.I. Khondaker and S. Seal, Progr. Mater. Sci., 2011, **56**, 1178–1271.
16. S. Bai and X. Shen, RSC Adv., 2012, **2**, 64–98.
17. X.Z. Tang, Z.W. Cao, H.B. Zhang, J. Liu and Z.Z. Yu, Chem. Commun., 2011, **47**, 3084–3086.
18. S. Kumar, C. Selvaraj, L. G. Scanlon and N. Munichandraiah, Phys. Chem. Chem. Phys., 2014, **16**, 22830–22840.
19. L. Yu, Y. Zhang, B. Zhang and J. Liu, Sci. Rep. 2014, **4**, doi:10.1038/srep04551.
20. W.P. Xu, L.C. Zhang, J.P. Li, Y. Lu, H.H. Li, Y.N. Ma, W.D. Wang and S.H. Yu, J. Mater. Chem., 2011, **21**, 4593-4597
21. Y.L. Chen, Z.A. Hu, Y.Q. Chang, H.W. Wang, Z.Y. Zhang, Y.Y. Yang and H.Y. Wu, J. Phys. Chem. C 2011, **115**, 2563–2571.
22. S. Cui, S. Mao, Z. Wen, J. Chang, Y. Zhang and J. Chen, Analyst, 2013, **138**, 2877–2882.
23. J. Salamon, Y. Sathishkumar, K. Ramachandran, Y.S. Lee, D.J. Yoo, A.R. Kim and G. Gnana kumar, Biosens. Bioelectron., 2015, **64**, 269–276.
24. V. K. Sharma, R.A. Yngard and Y. Lin, Adv. Colloid Interface Sci., 2009, **145**, 83–96.
25. M. Rai, A. Yadav and A. Gade, Biotech. Adv., 2009, **27**, 76–83.
26. C. Karuppiah, S. Palanisamy, S.M. Chen, R. Emmanuel, M. Ajmal Ali, P. Muthukrishnan, P. Prakash and F.M.A. Al-Hemaid, J. Solid State Electrochem., 2014, **18**, 1847–1854.
27. R. Emmanuel, C. Karuppiah, S.M. Chen, S. Palanisamy, S. Padmavathy and P. Prakash, J. Hazard. Mater., 2014, **279**, 117–124.
28. S. Palanisamy, S.M. Chen and R. Sarawathi, Sens. Actuators B, 2012, **166–167**, 372–377.
29. L. Lina, W. Wang, J. Huang, Q. Li, D. Sun, X. Yang, H. Wang, N. He and Y. Wang, Chemical J., 2010, **16**, 852–858.
30. U. Schillinger and F.K. Lucke, Appl. Environ. Microbiol., 1989, **55**, 1901–1906.
31. A. Doss, V. Parivuguna, M.V. Santhi and S. Surendran, Indian J. Sci. Tech., 2011, **4**, 550–552.
32. H.M. Mubarack, A. Doss, R. Dhanabalan and R. Venkataswamy, J. Animal Vet. Ad., 2011, **10**, 738–741.
33. P. Li, J. Li, C. Wu, Q. Wu and J. Li, Nanotechnology 2005, **16**, 1912–1917.
34. P.I. Alade and O.N. Irobi, J. Ethnopharcol., 1993, **39**, 171–174.
35. V.G. Kumara, S.D. Gokavarapu, A. Rajeswari, T.S. Dhas, V. Karthick, , Z. Kapadia, T. Shrestha, I.A. Barathy, A. Roy and S. Sinha, Colloids Sur. B, 2011, **87**, 159–163.

Journal Name

View Article Online
DOI: 10.1039/C5RA00992H ARTICLE

36. V. Wiskam, W. Fichtner, V. Kramb, A. Nintschew and J.S. Schneider, J. Chem. Educ. 1995, **722**, 952–954.

37. Y.P. Li, H.B. Cao, C.M. Liu and Y. Zhang, J. Hazard. Mater., 2007, **148**, 158–163.

38. X. Zhou, C. Yuan, D. Qin, Z. Xue, Y. Wang, J. Du, L. Ma, L. Ma and X. Lu, Electrochim. Acta, 2014, **119**, 243–250.

39. P.K. Rastogi, V. Ganesan and S. Krishnamoorthi, Electrochim. Acta, 2014, **147**, 442–450.

40. M. Najafiz and M. Sadeghi, ECS Electrochem. Lett., 2013, **2**, H5-H8.

41. G. Kokkinidis and K. Juttner, Electrochim. Acta, 1981, **26**, 971–977.

42. B. Qi, F. Lin, J. Bai, L. Liu and L. Guo, Mater. Lett., 2008, **62**, 3670-3672.

43. L. Luo, X. Wang, Y. Ding, Q. Li, J. Ji and D. Deng, Anal. Methods, 2010, **2**, 1095-1100.

44. F. Liang, B. Liu, Y. Deng, S. Yang and C. Sun, Microchim. Acta, 2011, **174**, 407-412.

45. Y. Zhang, L. Zeng, X. Bo, H. Wang and L. Guo, Anal. Chim. Acta, 2012, **752**, 45-52.

46. Y. Zhang, X. Bo, A. Nsabimana, C. Luhana, G. Wang, H. Wang, M. Li and L. Guo, Biosens. Bioelectron. 2014, **53**, 250-256.

47. Z. Xue, H. Lian, C. Hu, Y. Feng, F. Zhang, X. Liu and X. Lu, Aust. J. Chem., dx.doi.org/10.1071/CH13607.

48. P.K. Rastogi, V. Ganesan, S. Krishnamoorthi, Electrochim. Acta, 2014, **147**, 442–450.

View Article Online
DOI: 10.1039/C5RA00992H Journal Name

Table 1 Comparison of the analytical parameters (linear range, sensitivity and LOD) of proposed GO-AgNPs modified electrode with other modified electrodes for the determination of NB.

Modified electrode	Linear range (μM)	Sensitivity ($\mu A \mu M^{-1} cm^{-2}$)	LOD[a] (μM)	Ref.
OMC[b]/DDAB[c]/GCE[d]	20–2900	–	10	[42]
BiF[e]/CPE[f]	1–100	0.289	0.83	[43]
ATP-Ag[g]/GCE	3–30	–	1.1	[44]
PNMPC[h]/Nafion/GCE	1–200	6.93	0.05	[45]
OMCN[i]/GCE	0.5–1000	0.675	0.18	[46]
TMPP[j]/N-OMC[k]/GCE	0.528–132	–	0.38	[47]
Pd[l]-GG-g-PAM[m]-silica/GCE	1–3900	0.026	0.06	[48]
RGO[n]-AgNPs[o]/GCE	0.5–900	0.836	0.26	Present work

[a]LOD – limit of detection; [b]OMC – ordered mesoporus carbon; [c]DDAB – didodecyldimethylammonium bromide; [d]GCE – glassy carbon electrode; [e]BiF – bismuth-film; [f]CPE – carbon paste electrode; [g]ATP-Ag – attapulgite-silver nanocomposites; [h]PNMPC – platinum nanoparticles/macroporous carbon; [i]OMCN – ordered mesoporous carbon nitride; [j]TMPP – tetra(4-methoxyphenyl) porphyrin; [k]N-OMC – N-doped ordered mesoporous carbon; [l]Pd – palladium nanoparticles; [m]GG-g-PAM – guar gum grafted polyacrylamide; [n]RGO – reduced graphene oxide; [o]AgNPs – silver nanoparticles.

Sample	Added (μM)	Found[a] (μM)	Recovery (%)	RSD[b] (%)
Waste water 1	15	15.13	100.8	2.96
Waste water 2	30	29.82	99.4	2.63
Waste water 3	60	58.97	98.2	3.22

Table 2 Electrochemical determination of NB in waste water samples using RGO-AgNPs/GCE by DPV. (n=3)

[a]Standard addition method; [b]Relative standard deviation of three measurements.